CARDIFF UNIVERSITY
PRIFYSGOL CAERDYDD

ORCA – Online Research @ Cardiff

This is an Open Access document downloaded from ORCA, Cardiff University's institutional repository:https://orca.cardiff.ac.uk/id/eprint/131048/

This is the author's version of a work that was submitted to / accepted for publication.

Citation for final published version:

Sun, Xi, Dawson, Simon R., Parmentier, Tanja E., Malta, Grazia, Davies, Thomas E., He, Qian , Lu, Li, Morgan, David J. , Carthey, Nicholas, Johnston, Peter, Kondrat, Simon A., Freakley, Simon J., Kiely, Christopher J. and Hutchings, Graham J. 2020. Facile synthesis of precious-metal single-site catalysts using organic solvents. Nature Chemistry 12 , pp. 560-567. 10.1038/s41557-020-0446-z

Publishers page: http://dx.doi.org/10.1038/s41557-020-0446-z

Please note:
Changes made as a result of publishing processes such as copy-editing, formatting and page numbers may not be reflected in this version. For the definitive version of this publication, please refer to the published source. You are advised to consult the publisher's version if you wish to cite this paper.

This version is being made available in accordance with publisher policies. See http://orca.cf.ac.uk/policies.html for usage policies. Copyright and moral rights for publications made available in ORCA are retained by the copyright holders.

Supplementary Information

Facile synthesis of precious-metal single-site catalysts using organic solvents

Xi Sun[a,b,†], Simon R. Dawson[a,†], Tanja E. Parmentier[a], Grazia Malta[a], Thomas E. Davies[a], Qian He[a], Li Lu[c], David J. Morgan[a], Nicholas Carthey[d], Peter Johnston[e], Simon A. Kondrat[a,f], Simon J. Freakley[a,g], Christopher J. Kiely[a,c] and Graham J. Hutchings*[a]

[a] *Cardiff Catalysis Institute, School of Chemistry, Cardiff University, Main Building, Park Place, Cardiff, CF10 3AT, U.K.*

[b] *Department of Chemistry, Lanzhou University, Lanzhou 730000, China.*

[c] *Department of Materials Science and Engineering, Lehigh University, 5 East Packer Avenue, Bethlehem, PA 18015, USA.*

[d] *Johnson Matthey Technology Centre, Blounts Court, Sonning Common, RG4 9NH, U.K.*

[e] *Process Technologies, Johnson Matthey PLC, Billingham, TS23 1LB, U.K.*

[f] *Department of Chemistry, Loughborough University, Loughborough, Leicestershire, LE11 3TU, U.K.*

[g] *Department of Chemistry, University of Bath, Claverton Down, Bath BA2 7AY, U.K.*

† *These authors contributed equally to this work*

*Hutch@cf.ac.uk

Table of Contents

Supplementary Table 1 – EXAFS fitting of metal acetylacetonate standards and fresh catalysts 1

Supplementary Table 2 – List of catalysts prepared using various solvents and drying temperatures with a nominal metal loading of 1wt.% Au. 2

Supplementary Table 3 – EXAFS fitting of Au/C-acetone catalyst before and after reaction at 200 ºC along with comparison of the conventional 1wt.% Au/C-AR catalyst. 3

Supplementary Table 4 – EXAFS modelling for the Au L_3-edge of the 1wt.% Au/C-Acetone samples at different times-on-line and gas environments at 180 ºC. 4

Supplementary Table 5 – *Ex situ* EXAFS 1st shell-fitting of the 1wt.% Pd catalysts at various stages of reaction. 5

Supplementary Table 6 – *Ex situ* EXAFS 1st shell-fitting of the 1wt.%Pt catalysts at various stages of reaction. 6

Supplementary Table 7 – *Ex situ* EXAFS 1st shell fitting of the 1wt.% Ru catalysts at various stages of reaction. 7

Supplementary Figure 1 – XRD pattern of the carbon support. 8

Supplementary Figure 2 – XPS analysis of the carbon support. 9

Supplementary Figure 3 – XAS analysis of the freshly prepared 1 wt.% Au/C-Acetone catalyst. 10

Supplementary Figure 4 – XAS characterisation of the freshly prepared 1wt.% Pd/C-Acetone catalyst. 11

Supplementary Figure 5 – XAS characterisation of the freshly prepared 1wt.% Pt/C-Acetone catalyst. 12

Supplementary Figure 6 – XAS characterisation of the freshly prepared 1wt.% Ru/C-Acetone catalyst. 13

Supplementary Figure 7 – High angle annular dark field (HAADF) images of the 1wt.% Pd/C, 1wt.% Pt/C and 1wt.% Ru/C catalysts prepared using acetone. 14

Supplementary Figure 8 – X-ray diffraction patterns of the 1wt.% Au/C catalysts prepared using various solvents (with high boiling points and drying temperatures). 15

Supplementary Figure 9 – Time-on-line acetylene hydrochlorination activity profiles of the Au/C-Acetone, Au/C-*aqua regia* and Au/C-H_2O catalysts. 16

Supplementary Figure 10 – X-ray diffraction patterns of the fresh 1wt.% Au/C-Acetone catalyst (fresh), after 4h of reaction (used 4 h) and after a further 3 h of reaction (used 7 h). 17

Supplementary Figure 11 – *In situ* XRD analysis of the Pd/C, Pt/C and Ru/C catalysts prepared using acetone. 18

Supplementary Figure 12 – X-ray diffraction patterns of the 1wt.% Pd/C and Ru/C catalysts prepared with acetone and water-soluble metal precursors. 19

Supplementary Figure 13 – FT-EXAFS analysis of the Pd/C, Pt/C and Ru/C catalysts prepared using acetone. 20

Supplementary Figure 14 – Correlation of coordination numbers (CN) of Au/C-Acetone during acetylene hydrochlorination at 180 °C as determined from EXAFS fitting and XANES linear combination fitting (LCF-XANES). 21

Supplementary Figure 15 – High angle annular dark field (HAADF) images of the 1wt.% Au/C, 1wt.% Pd/C, 1wt.% Pt/C and 1wt.% Ru/C catalysts prepared using acetone at different time-on-line and gas environment. 22

Supplementary Figure 16 – XPS spectra of the 1wt.% Pd/C, 1wt.% Pt/C and 1wt.% Ru/C catalysts prepared using acetone after reaction..... 23

Supplementary Table 1 – EXAFS fitting of metal acetylacetonate standards and fresh catalysts

Sample	Paths	CN	R (Å)	$2\sigma^2$(Å^2)	$So_2^{\#}$	E_f(eV)	R_{factor}
$Pd(acac)_2$ std	Pd-O	4*	1.98(1)	0.0015(13)	0.9	4(1)	0.013
	Pd-C	4*	2.94(5)	0.0085(82)			
1wt%. $Pd(acac)_2$/C	Pd-O	4.9(5)	1.98*	0.004(1)	0.9*	5.0(6)	0.0126
	Pd-C	4.9$^{\$}$	2.97(5)	0.019 (10)			
Fitting parameters	k-range: 3-12.5 Å^{-1}			R-range:1.1-2.5 Å			
$Pt(acac)_2$ std	Pt-O	4*	1.98(1)	0.0010(9)	0.75	8(2)	0.0203
	Pt-C	4*	2.89(4)	0.0019(4)			
	Pt-O-C	8*	3.16(13)	0.005(2)			
1wt%. $Pt(acac)_2$/C	Pt-O	3.8(6)	1.98(1)	0.005(1)	0.75*	8(2)	0.0240
	Pt-C	3.8(6)$^{\$}$	2.89(4)	0.0018(44)			
	Pt-O-C	8*	3.20(20)	0.015$^{\wedge}$			
Fitting parameters	k-range: 2.25-10 Å^{-1}			R-range:1.1-2.5 Å			
$Ru(acac)_3$ std$^{\&}$	Ru-O	6*	2.01(6)	0.0020(8)	0.9*	1(2)	0.029
1wt%. $Ru(acac)_3$/C$^{\&}$	Ru-O	6.2(9)	2.01(1)	0.002(1)	0.9	1(2)	0.024
Fitting parameters	k-range: 3-12.5 Å^{-1}			R-range:1-2.5 Å			

$^{\#}$ Amplitude reduction factors determined from fitting of metal (acac) standards with fixed coordination numbers as determined from FEFF calculations.

* Values fixed in fit.

$^{\$}$ M-C CN values set as equal to determined M-O CN.

$^{\wedge}$ $2\sigma^2$ set as 1st shell value x5.

$^{\&}$ Due to a large number pathlengths in $Ru(acac)_3$ including strong multiple scattering features it was not possible to satisfactorily fit beyond the first Ru-O shell.

Supplementary Table 2 – List of catalysts prepared using various solvents and drying temperatures with a nominal metal loading of 1wt.% Au.

Wherever extra dry solvents were used, the catalysts are denoted (dry).

Catalysts	Polarity ($E_T(30)$)[24]	Boiling Point (°C)	Drying temperature (°C)
Au/C-H_2O	63.1	100	105
Au/C-MeOH-(dry)	55.5	64.8	70
Au/C-EtOH-(dry)	51.8	78.3	85
Au/C-1-Propanol	50.7	97.1	105
Au/C-1-Butanol	50.2	117.7	120
Au/C-2-Propanol-(dry)	48.6	82.4	90
Au/C-2-Butanol-(dry)	47.1	107.9	110
Au/C-Acetone-(dry)	42.2	56.5	40
Au/C-2-Butanone-(dry)	41.3	79.6	85
Au/C-Ethyl Acetate-(dry)	38.1	77.1	85
Au/C-Diethyl Ether	34.6	34.6	45
Au/C-THF-(dry)	37.4	66.0	70
Au/C-DMSO	45.0	189	195
Au/C-DMF	43.8	154	160
Au/C-Cyclohexanone	40.8	155	160
Au/C-*Aqua Regia*			140

Supplementary Table 3 – EXAFS fitting of Au/C-acetone catalyst before and after reaction at 200 ºC along with comparison of the conventional 1wt.% Au/C-AR catalyst.

Sample	Paths	CN	R (Å)	$2\sigma^2$(Å^2)	So_2[#]	E_f(eV)	R_{factor}
Au/C-Ar	Au-Cl	2.58 (8)	2.273(4)	0.0011(5)	0.75	2.8(7)	0.006
Au/C-acetone	Au-Cl	2.31(8)	2.269(2)	0.0023(3)		8.9(4)	0.0059
Au/C-acetone used catalyst	Au-Cl	2.0(1)	2.267(4)	0.0025(5)		8.1(5)	0.011
	Au-Au	1.6(1)	2.877(11)	0.008(2)			
$KAuCl_4$ std	Au-Cl	4*	2.284(3)	0.0011(5)		2.9(5)	0.014
Au_2O_3 std	A-O	4*	1.99(6)	0.0028(4)		7.1(7)	0.014

Fitting parameters: k = 3-16 (Å^{-3}); R range 1.15-3

Note: On the basis that Au(0) is present as large particles with a Au-Au CN of 12, the calculated CN numbers for the Au/C-Acetone used catalyst can be re-calculated as fractions of $AuCl_x$ and Au(0). Using the values from LCF analysis in Figure 3b an average Au-Cl CN value of 2.3 was taken (reflecting a mixture of Au(III) and Au(I). Based on these two assumed actual CN values the fraction of Au(0) within the sample, as determined by EXAFS is 13%. This value is in good agreement with the 14% determined by LCF of XANES.

Supplementary Table 4 – EXAFS modelling for the Au L_3-edge of the 1wt.% Au/C-Acetone samples at different times-on-line and gas environments at 180 ºC.

Model	Paths	CN	Path length	$2\sigma^2$	So_2	Enot	R factor
Fresh catalyst	Au-Cl	2.4(1)	2.263(5)	0.0025(5)	0.75	6.2(7)	0.0141
Heated to 180 °C in Ar	Au-Cl	2.3(2)	2.267(5)	0.0021(5)	0.75	8.1(8)	0.0182
Heated to 180 °C in HCl	Au-Cl	2.7(2)	2.270(6)	0.0021(6)	0.75	8.7(9)	0.0332
After 5 min reaction	Au-Cl	2.6(2)	2.270(5)	0.0030(6)	0.75	7.8(7)	0.0228
After 240 min reaction	Au-Cl	2.9 (2)	2.281(5)	0.0037(5)	0.75	8.1(7)	0.0197

Fitting parameters: k = 3-16 ($Å^{-3}$); R 1.15-3

Supplementary Table 5 – *Ex situ* EXAFS 1st shell-fitting of the 1wt.% Pd catalysts at various stages of reaction. Catalysts under reaction conditions have been fitted with 2 models namely (1) Pd-Cl only; (2) Pd-Cl and Pd-O. Green background colouring indicates viable fitting, whereas red background fits are considered unviable.

Sample	Paths	CN	R (Å)	$2\sigma^2$(Å^2)	So_2[#]	E_f(eV)	R_{factor}
1wt%. $Pd(acac)_2$/C fresh	Pd-O	5.4(6)	1.98(1)	0.005(2)	0.9	4(1)	0.021
1wt%. $Pd(acac)_2$/C 180 ° C under Argon	Pd-O	4.4(7)	1.98(1)	0.0022(16)		3(2)	0.029
1wt%. $Pd(acac)_2$/C 180 ºC initial VCM (fit 1)	Pd-Cl	3.6(4)	2.30(1)	0.007(1)		1(1)	0.017
1wt%. $Pd(acac)_2$/C 180 ºC initial VCM (fit 2)	Pd-O	3.7(1.2)	2.15(4)	0.010(5)		12(3)	0.009
	Pd-Cl	2.3(9)	2.35(2)	0.007(4)			
1wt%. $Pd(acac)_2$/C 180 ºC 240 min VCM (fit 1)	Pd-Cl	3.5(3)	2.31(1)	0.008(1)		0(1)	0.016
1wt%. $Pd(acac)_2$/C 180 ºC 240 min VCM (fit 2)	Pd-O	3.8(9)	2.17(4)	0.010(4)		11(2)	0.0047
	Pd-Cl	2.4(8)	2.35(1)	0.009(4)			
$PdCl_2$ std.	Pd-Cl	4*	2.313(8)	0.0031(6)		4(1)	0.0135
Fitting parameters	k-range: 3-12.5 Å^{-1}			R-range:1.1-2.5 Å			

Note: Fitting of multiple Pd-O and Pd-Cl paths (fitting model 2) for the catalysts under reaction conditions was considered unviable, despite improved R_{factor} values, due to high CN values, high changes in E_f. and unrealistic lengthening of the Pd-O pathlength.

Amplitude reduction factor determined from metal acetylacetonate standards.

Supplementary Table 6 – *Ex situ* EXAFS 1st shell-fitting of the 1wt.%Pt catalysts at various stages of reaction. Catalysts under reaction conditions have been fitted with 2 models. (1) Pt-Cl only; (2) Pt-Cl and Pt-O. Green background colouring indicates viable fitting.

Sample	Paths	CN	R (Å)	$2\sigma^2$(Å^2)	So_2#	E_f(eV)	R_{factor}
1wt%. $Pt(acac)_2$/C fresh	Pt-O	4.1(5)	1.98(2)	0.001*	0.75	8(3)	0.029
1wt%. $Pt(acac)_2$/C 180 ° C under Argon	Pt-O	4.2(3)	1.99(1)	0.002*		7(2)	0.016
1wt%. $Pt(acac)_2$/C 180 ºC initial VCM (fit 1)	Pt-Cl	4.6(7)	2.27(2)	0.010(2)		1(1)	0.015
1wt%. $Pt(acac)_2$/C 180 ºC initial VCM (fit 2)	Pt-O	1.0(3)	1.99*	0.002*		4(1)	0.009
	Pt-Cl	3.1(3)	2.30(1)	0.006*			
1wt%. $Pt(acac)_2$/C 180 ºC 240 min VCM (fit 1)	Pt-Cl	3.5(3)	2.32(7)	0.003(3)		8(3)	0.035
$PtCl_4$	Pt-Cl	4*	2.28(1)	0.003(1)		2(2)	0.018
Fitting parameters	k-range: 2.25-10 Å^{-1}			R-range:1.1-2.5 Å			

Note: Fitting of Pt-Cl only (model 1) or Pt-O and Pt-Cl (model 2) to the catalyst after initial VCM reaction was considered equally valid. Model 2 reflects residual $Pt(acac)_2$ (~25%- acac, assuming a $PtCl_4$ chloride species). The catalyst after 240 min reaction time could not be fitted with a valid Pt-O pathlength (So_2 values found to be negative).

Amplitude reduction factor determined from metal acetylacetonate standards.

*Fixed parameters

Supplementary Table 7 – *Ex situ* EXAFS 1st shell fitting of the 1wt.% Ru catalysts at various stages of reaction. Catalysts under reaction conditions have been fitted with 2 models. (1) Ru-Cl only; (2) Ru-Cl and Ru-O. Green background colouring indicates viable fitting, while red background fits have been considered unviable.

Sample	Paths	CN	R (Å)	$2\sigma^2$(Å^2)	So_2#	E_f(eV)	R_{factor}
1wt%. $Ru(acac)_3$/C fresh	Ru-O	6.2(9)	2.01(1)	0.0022(15)	0.9	1(2)	0.024
1wt%. $Ru(acac)_3$/C 180 ºC under Argon	Ru-O	5.9(8)	2.02(1)	0.0044(16)		2(2)	0.024
1wt%. $Ru(acac)_3$/C 180 ºC initial VCM (fit 1)	Ru-Cl	4.1(5)	2.38(1)	0.0078(18)		2(1)	0.029
1wt%. $Ru(acac)_3$/C 180 ºC initial VCM (fit 2)	Ru-O	1.0*	2.12(4)	0.004*		5(2)	0.023
	Ru-Cl	3.2(6)	2.40(2)	0.0061(23)			
1wt%. $Ru(acac)_3$/C 180 ºC 240 min VCM (fit 1)	Ru-Cl	3.8(1.0)	2.42(3)	0.003(3)		4(3)	0.129
1wt%. $Ru(acac)_3$/C 180 ºC 240 min VCM (fit 2)	Ru-O	1.0*	2.22(25)	0.004*		7(5)	0.103
	Ru-Cl	3.6(3.3)	2.43(5)	0.007(9)			
$RuCl_3$	Ru-Cl	6*	2.355(7)	0.0034(5)		2(1)	0.014
Fitting parameters	k-range: 3-12.5 Å^{-1}			R-range:1-2.5 Å			

Note: Fitting of multiple Ru-O and Ru-Cl paths (fitting model 2) for the catalysts under reaction conditions was considered unviable, despite improved R_{factor} values, due to unrealistic lengthening of the Ru-O pathlengths.

Amplitude reduction factor determined from metal acetylacetonate standard.s

* Fixed parameters.

Supplementary Figure 1 – XRD pattern of the carbon support.

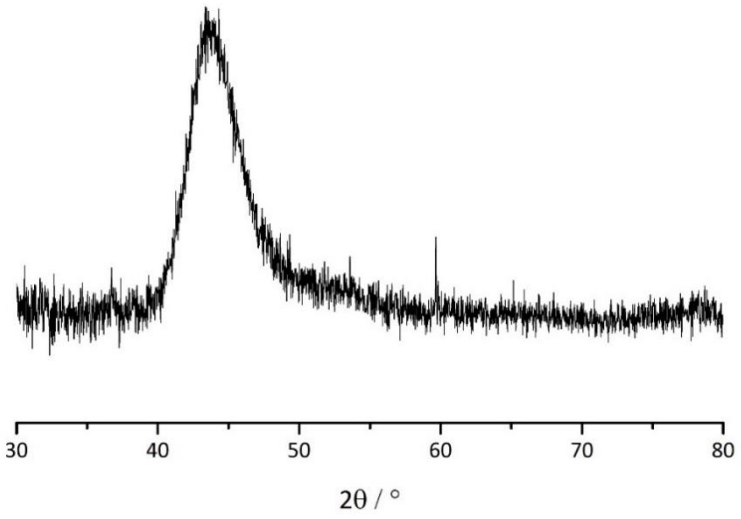

Supplementary Figure 2 – XPS analysis of the carbon support. a) a survey spectrum, b) the C(1s), c) the O(1s), d) the Cl(2p) and e) the S(2p) regions.

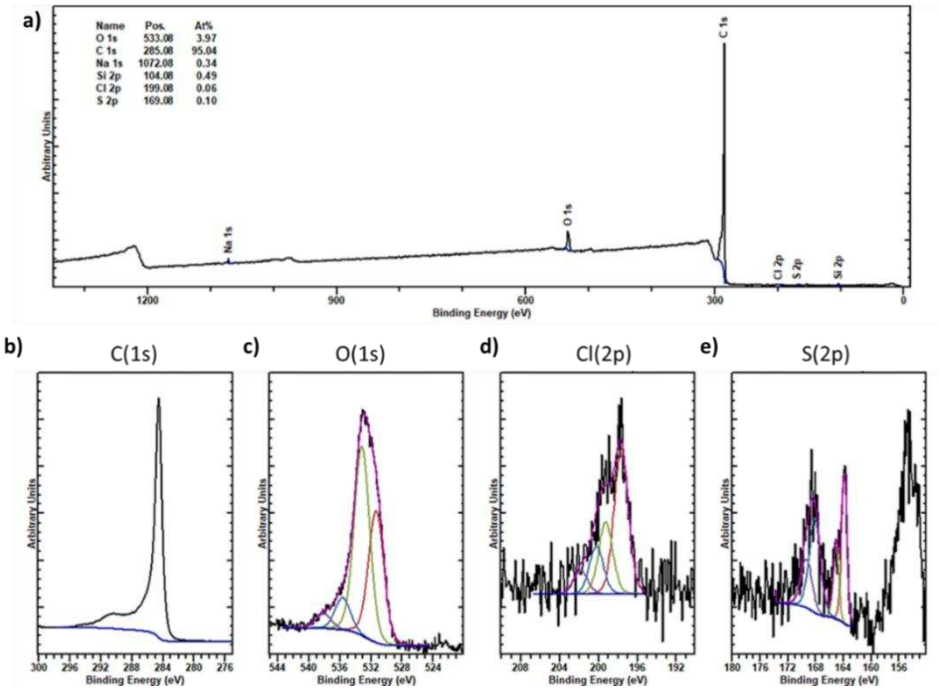

The carbon surface contains less than 5 at% oxygen, mostly as C-O-C/C-OH and carbonyl containing functional groups. The carbon also contains impurities including silicon, sodium, sulphur and chlorine at levels typically below 0.5 at%. The sulphur is present as SO_x and thiol functionalities, whilst the chlorine signal is comprised of C-Cl bonds (BE ~ 200 eV) and a species at *ca*. 198 eV, which we attribute to trace amounts of NaCl.

Supplementary Figure 3 – XAS analysis of the freshly prepared 1 wt.% Au/C-Acetone catalyst. a) Linear combination fitting (LCF) of the Au L_3-edge XANES and b) EXAFS modelling of 1wt% Au/C-Acetone (fresh) and associated standards ($KAuCl_4$ and Au_2O_3).

a

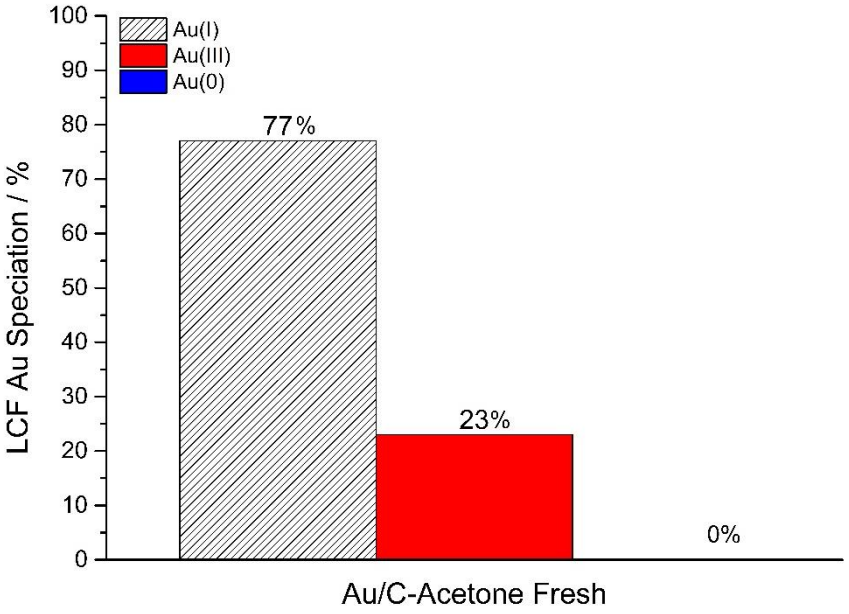

Au standards used: Au(III)/$[AuCl_4]^-$, Au(I)/$[AuCl_2]^-$ and Au(0)/Au Foil. $[AuCl_2]^-$ standard from difference spectra calculated in (1). R-Factor = 0.0014.

b

Model	Paths	CN	R (Å)	$2\sigma^2(Å^2)$	$So_2^{\#}$	E_f(eV)	R_{factor}
(1)	Au-Cl	2.31(8)	2.269(2)	0.0023(3)	0.75*	8.9(4)	0.0059
(2)	Au-Cl	2.6(5)	2.27(1)	0.0027(10)	0.75*	9.3(2.5)	0.0051
	Au-O	0.6(5)	2.24(25)	0.0027(10)			
(3)	Au-O	2.2(4)	2.16(6)	-0.001	0.75*	27.1(1.7)	0.1689
$KAuCl_4$ std	Au-Cl	4*	2.284(3)_	0.0011(5)	0.75(3)	2.9(5)	0.014
Au_2O_3 std	A-O	4*	1.99(6)	0.0028(4)	0.75*	7.1(7)	0.014

Fitting parameters: k = 3-16 ($Å^{-3}$); R range 1.15-3

1. Chang, S.-Y., Uehara, A., Booth, S. G., Ignatyev, K., Mosselmans, J. F. W., Dryfe , R. A. W., Schroeder, S. L. M., Structure and bonding in Au(I) chloride species: A critical examination of x-ray absorption spectroscopy (XAS) data. RSC Advances 5, 6912–6918 (2015).

Supplementary Figure 4 – XAS characterisation of the freshly prepared 1wt.% Pd/C-Acetone catalyst. Pd K-edge a) XANES and b) FT-EXAFS of the freshly prepared 1wt.% $Pd(acac)_2$/C-Acetone catalyst compared with the Pd foil and the $Pd(acac)_2$ standards.

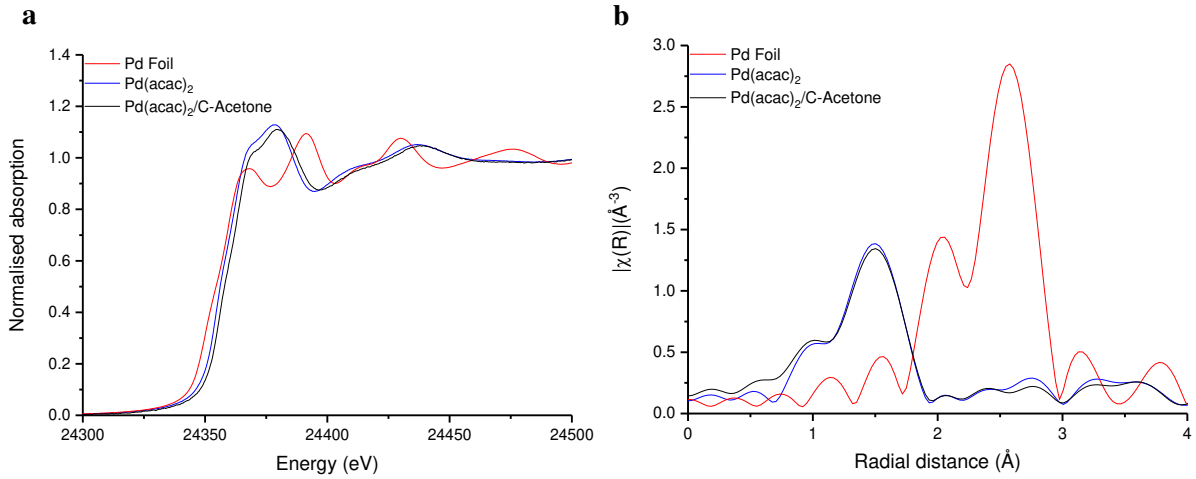

Supplementary Figure 5 – XAS characterisation of the freshly prepared 1wt.% Pt/C-Acetone catalyst. Pt L_3-edge a) XANES and b) FT-EXAFS of the freshly prepared 1wt.% $Pt(acac)_2$/C-Acetone catalyst compared with the Pt foil and the $Pt(acac)_2$ standards.

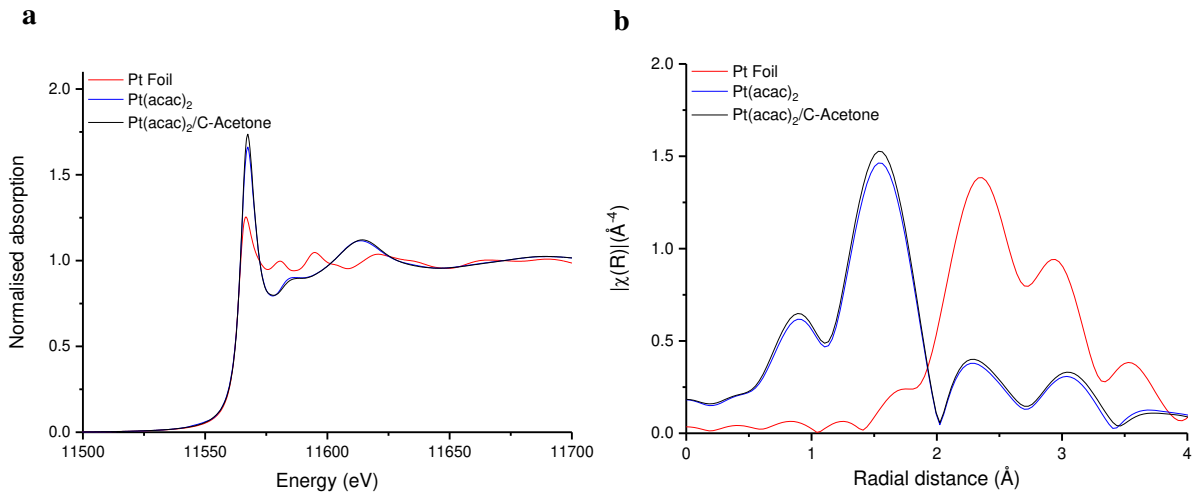

Supplementary Figure 6 – XAS characterisation of the freshly prepared 1wt.% Ru/C-Acetone catalyst. Ru K-edge a) XANES and b) FT-EXAFS of the freshly prepared 1wt.% $Ru(acac)_3$/C-Acetone catalyst compared with the Ru foil and the $Ru(acac)_3$ standards.

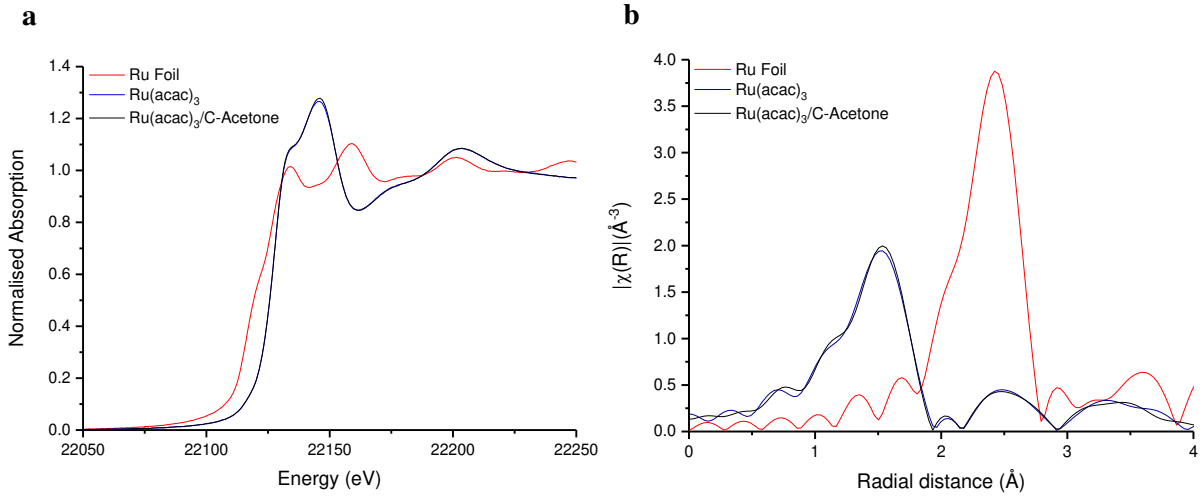

Supplementary Figure 7 – High angle annular dark field (HAADF) images of the 1wt.% Pd/C, 1wt.% Pt/C and 1wt.% Ru/C catalysts prepared using acetone. (a) and (b) are the higher magnification and lower magnification images of the 1wt.% Pd/C-Acetone catalyst, respectively, showing the presence of isolated Pd atoms and absence of larger Pd nanoparticles. (c) and (d) are the higher magnification and lower magnification images of the 1wt.% Pt/C-Acetone catalyst, respectively, showing the presence of isolated Pt atoms and absence of larger Pt nanoparticles. (e) and (f) are the higher magnification and lower magnification images of the 1wt.% Ru/C-Acetone catalyst, respectively, showing the presence of isolated Ru atoms and absence of larger Ru nanoparticles.

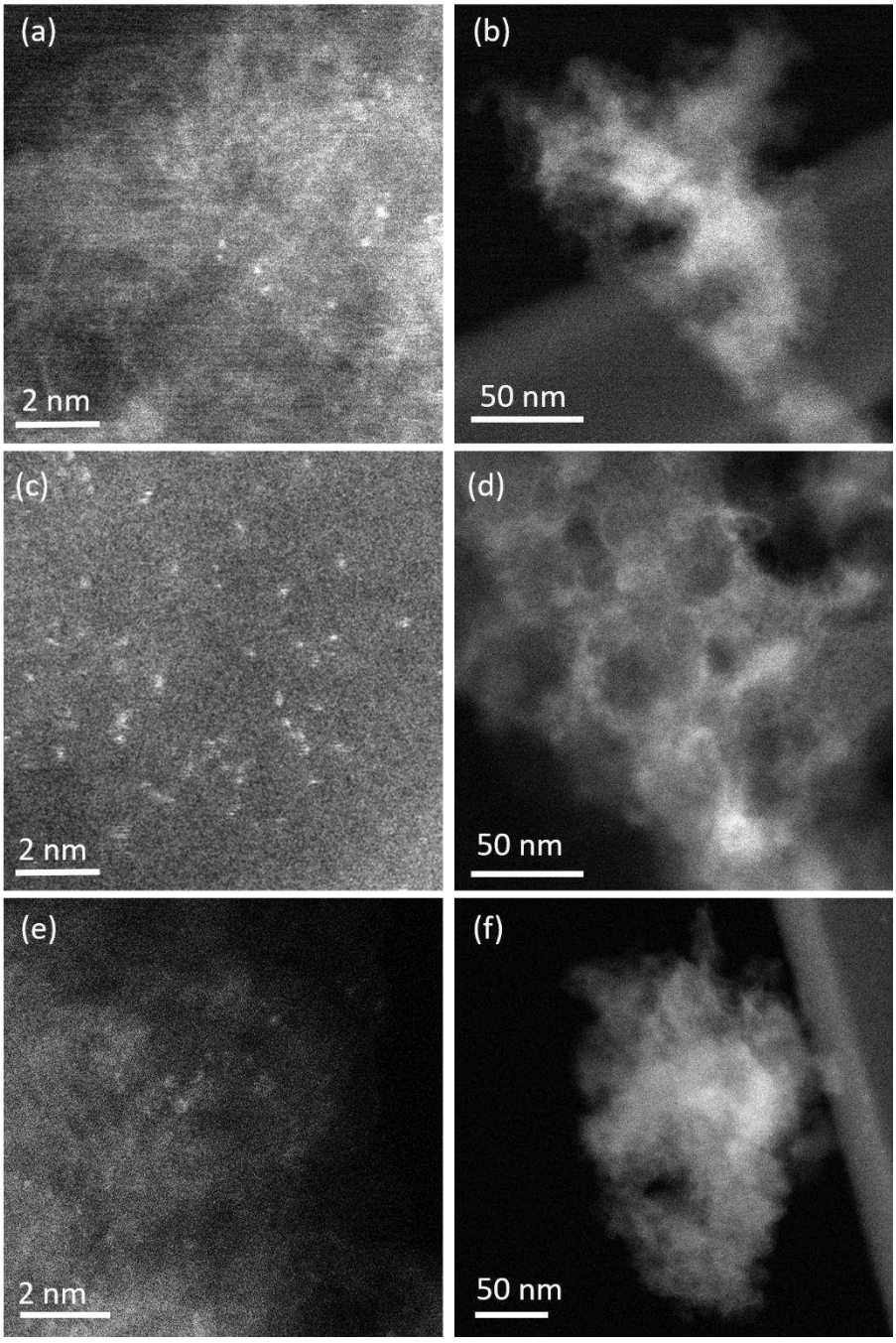

Supplementary Figure 8 – X-ray diffraction patterns of the 1wt.% Au/C catalysts prepared using various solvents (with high boiling points and drying temperatures).

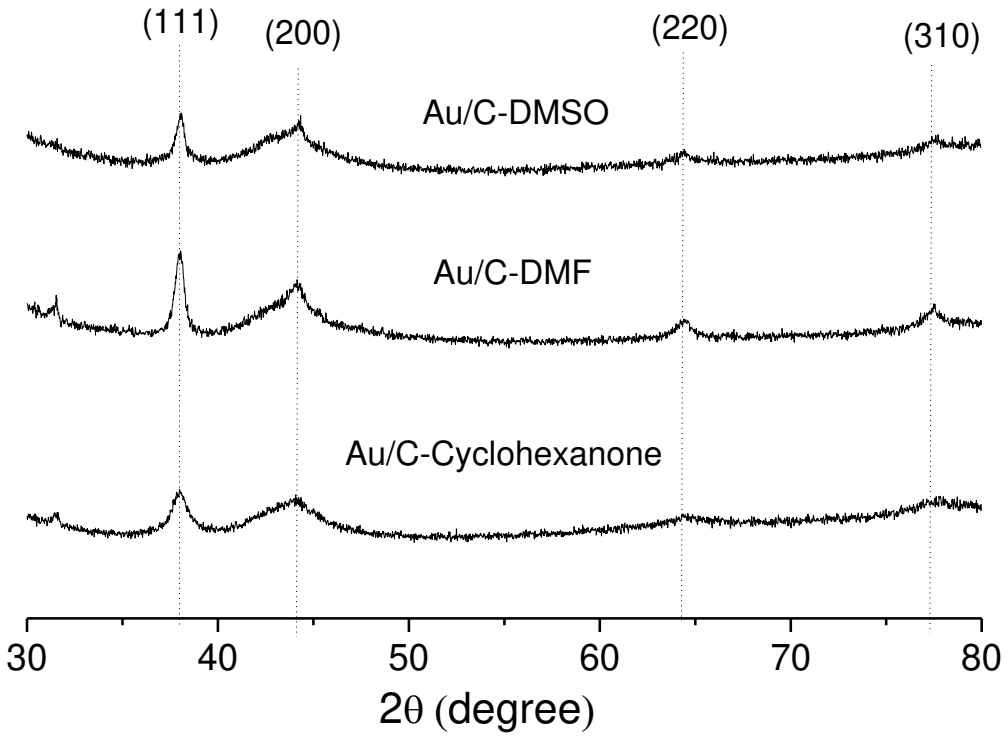

Supplementary Figure 9 – Time-on-line acetylene hydrochlorination activity profiles of the Au/C-Acetone, Au/C-*aqua regia* and Au/C-H_2O catalysts. Au/C-Acetone (▲), Au/C-*aqua regia* (●) and Au/C-H_2O (⬢) catalysts.

Test conditions: 90 mg catalyst, 23.5 mL min^{-1} C_2H_2, 23.7 mL min^{-1} HCl and 2.7 mL min^{-1} Ar, temperature 200 °C.

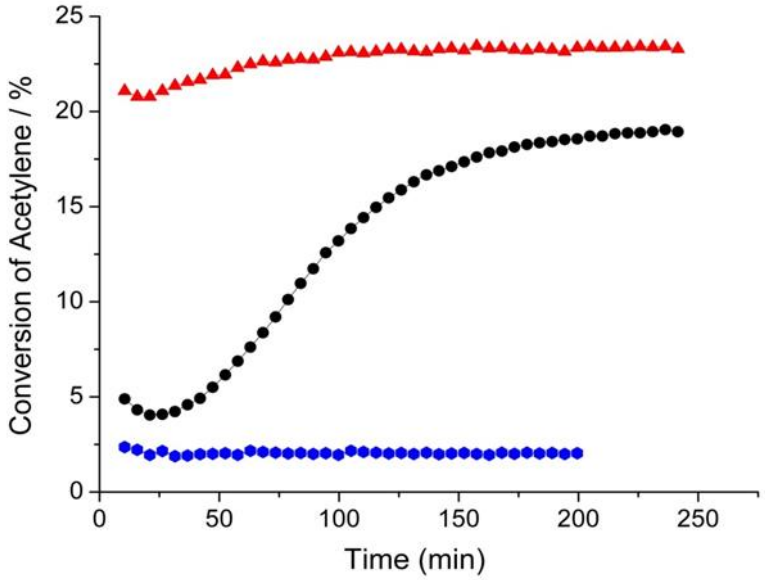

Supplementary Figure 10 – X-ray diffraction patterns of the fresh 1wt.% Au/C-Acetone catalyst (fresh), after 4h of reaction (used 4 h) and after a further 3 h of reaction (used 7 h).

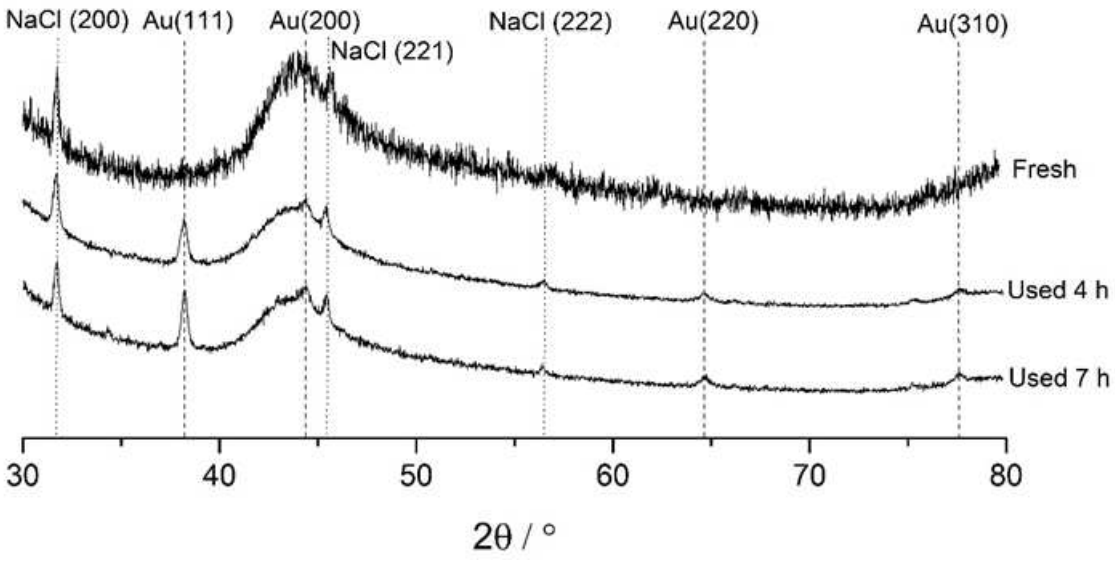

It is worth noting that weak reflections from NaCl could also be observed in the XRD patterns of these catalysts, especially when synthesized with ultra-dry solvents. This was attributed to the carbon support materials containing NaCl, which could easily recrystallize in the ultra-dry organic solvents. In aqueous solvents the NaCl can be both readily dissolved and well dispersed over the catalyst.

Supplementary Figure 11 – *In situ* XRD analysis of the Pd/C, Pt/C and Ru/C catalysts prepared using acetone. a) 1wt.% Au/c-acetone, b) 1wt.% $Pt(acac)_2$/c-acetone, c) 1wt.% $Pd(acac)_2$/c-acetone and d) 1wt.% $Ru(acac)_3$/c-acetone catalysts heated at a rate of 10°c/min under nitrogen (5 ml/min).

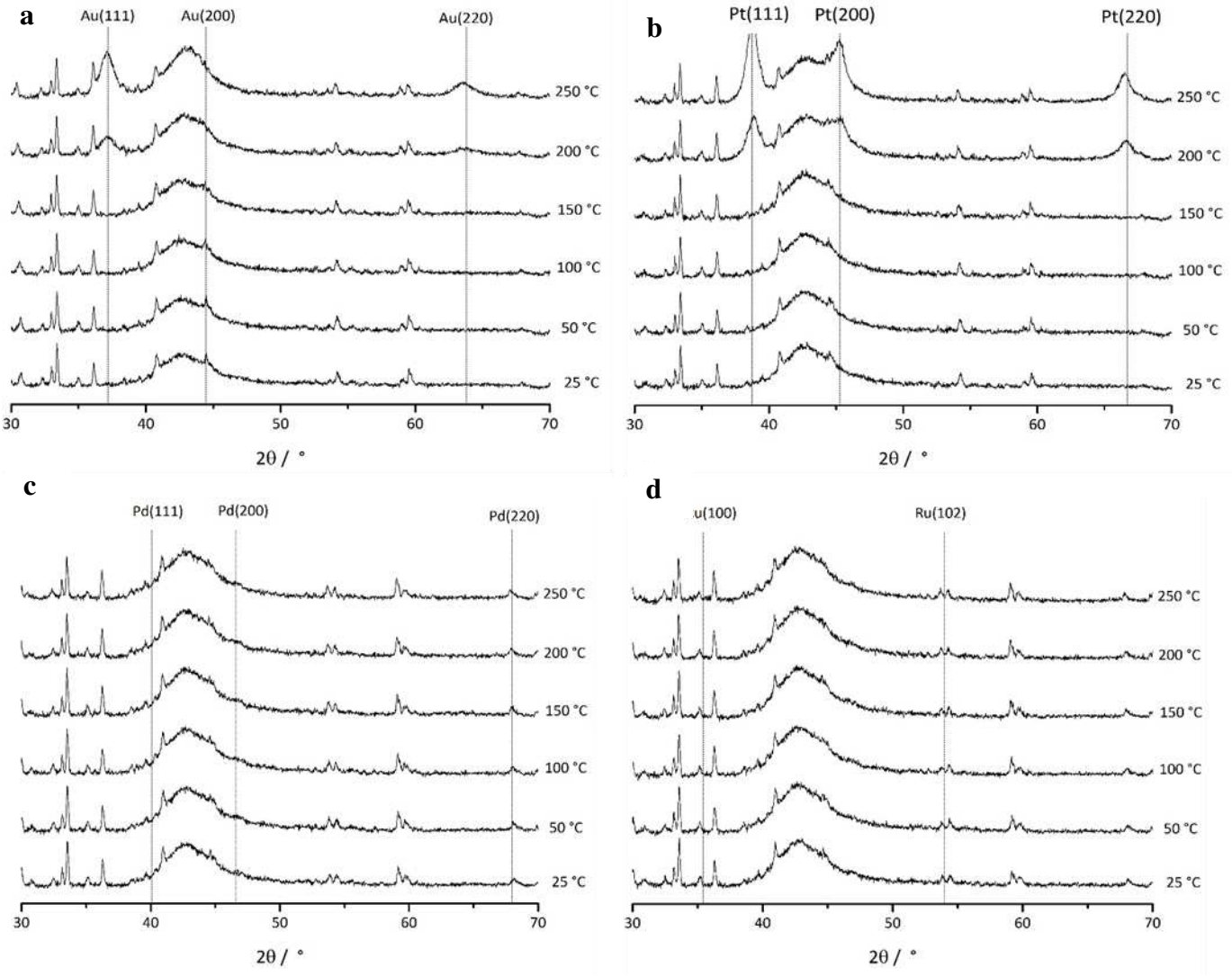

No reflections resulting from nanoparticle formation are observed in the diffractograms c) and d). Crystalline gold reflections can be seen in diffractogram a) above temperatures of 190°C and platinum nanoparticles can be detected in diffractogram b) from 190 °C upwards. Please note that the common reflections that can be seen in all the diffractograms are generated by the sample holder itself.

Supplementary Figure 12 – X-ray diffraction patterns of the 1wt.% Pd/C and Ru/C catalysts prepared with acetone and water-soluble metal precursors. a) $Pd(acac)_2$/C-acetone, b) $PdCl_2$/C-0.58M HCl catalysts, c) $Ru(acac)_3$/C-acetone and d) $RuCl_3$/C-H_2O in both the fresh state and after being heated up to 450 °C in an inert atmosphere.

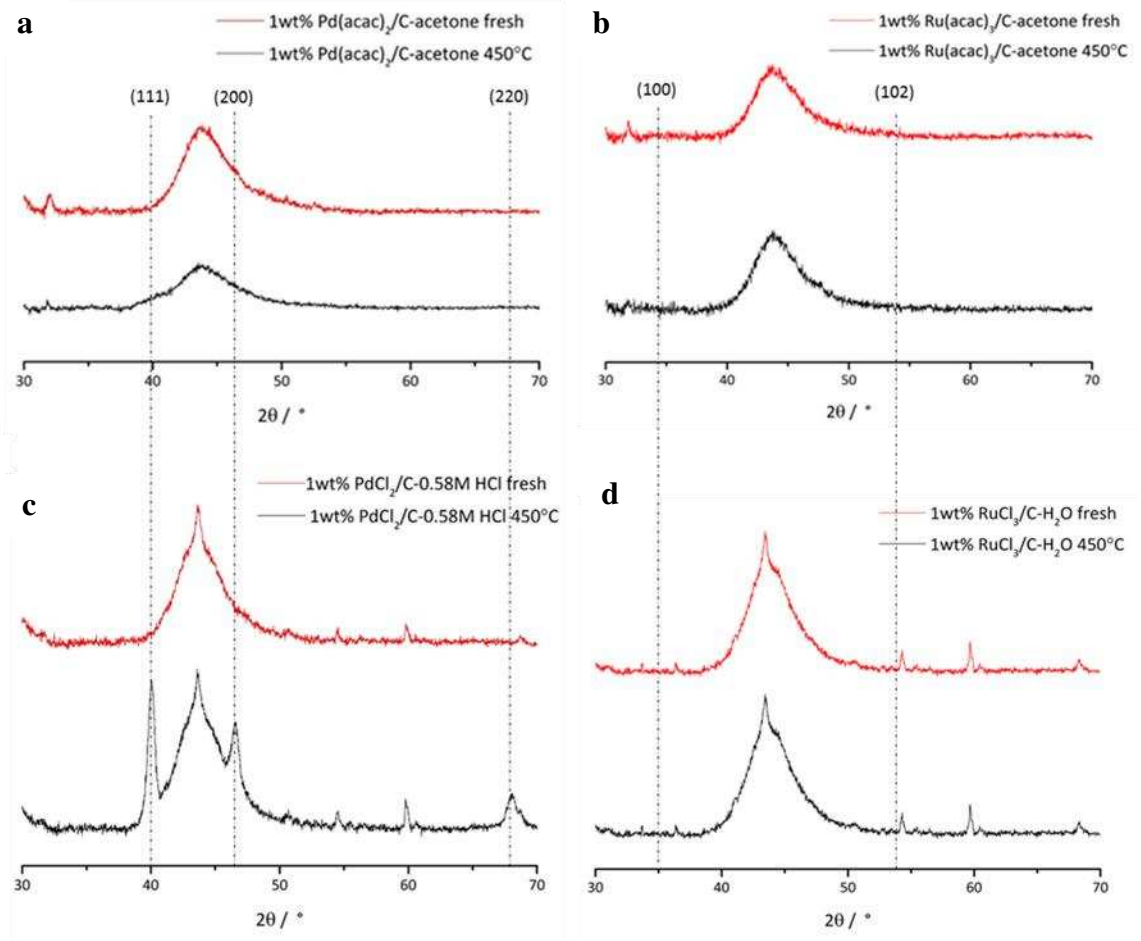

Supplementary Figure 13 – FT-EXAFS analysis of the Pd/C, Pt/C and Ru/C catalysts prepared using acetone. a) 1wt.% Au/C-Acetone, b) 1wt.% Pd/C-Acetone, c) 1wt.% Pt/C-Acetone and d) 1wt.% Ru/C-Acetone catalyst materials in their fresh and used states.

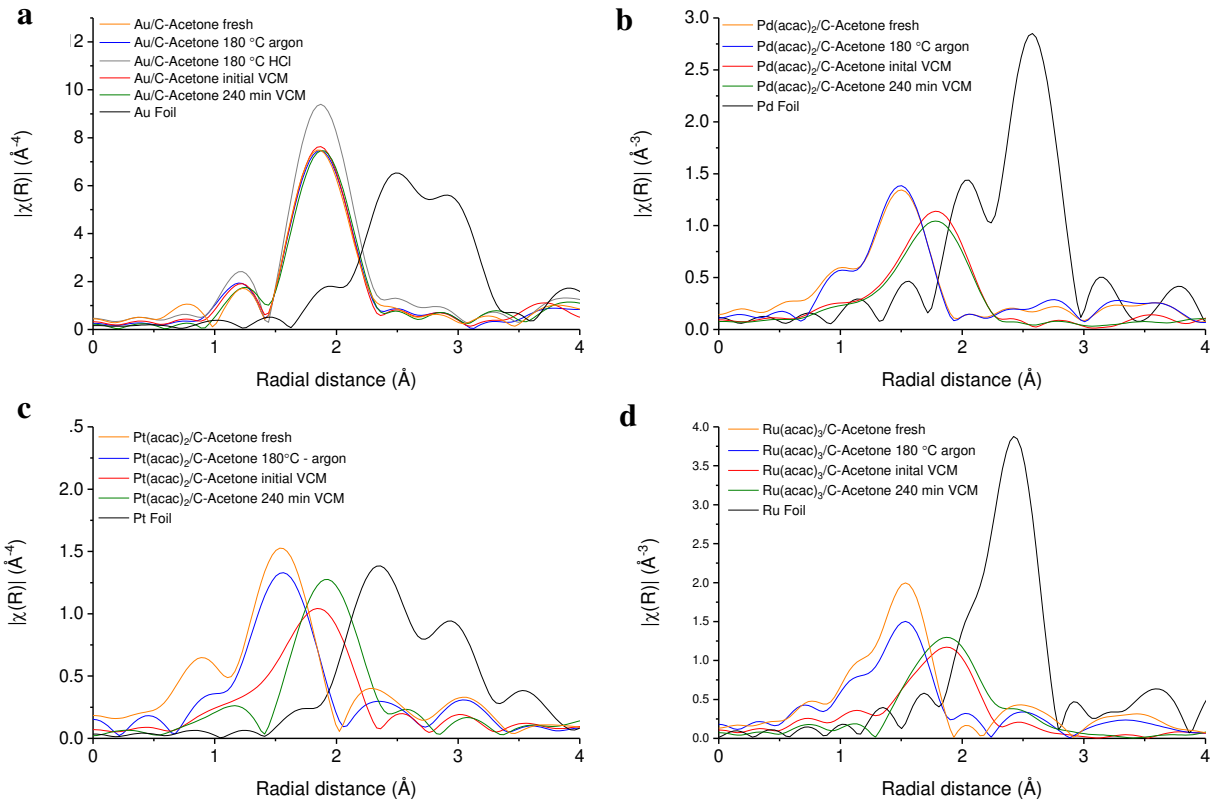

The Pt, Pd and Ru catalysts were found to be supported acetylacetonate complexes prior to testing. After reaction the local coordination changes from the $acac_x$ ligand to Cl^- analogous to that found for the Au catalyst. Importantly no metal-metal distances where observed in the EXAFS data.

Supplementary Figure 14 – Correlation of coordination numbers (CN) of Au/C-Acetone during acetylene hydrochlorination at 180 °C as determined from EXAFS fitting and XANES linear combination fitting (LCF-XANES).

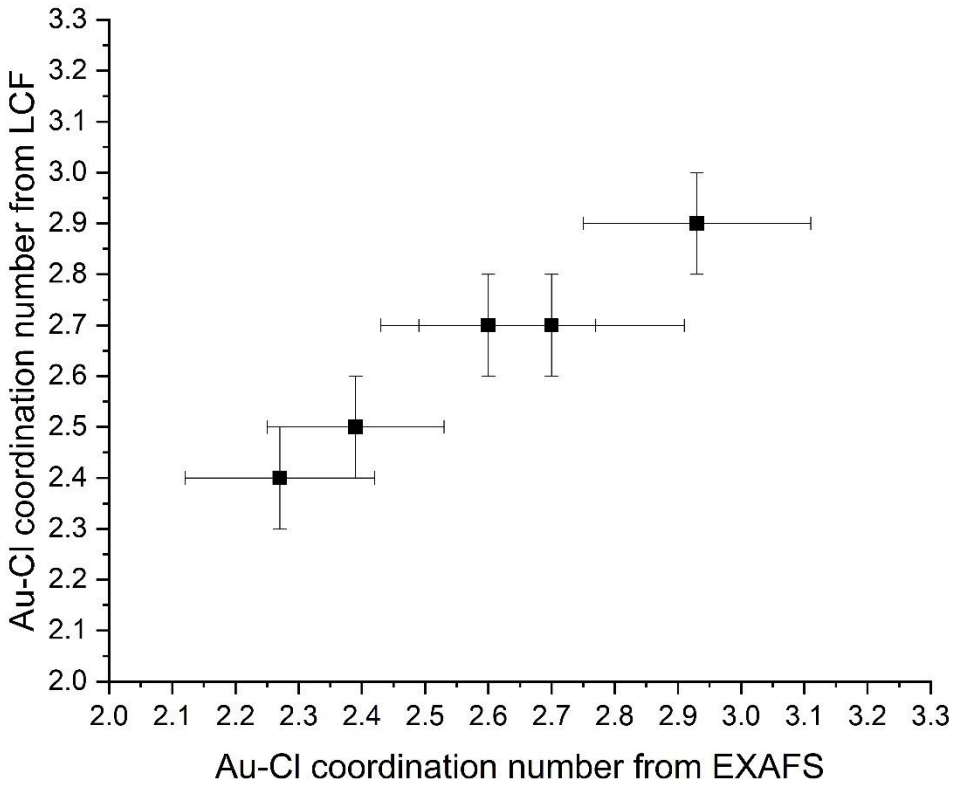

EXAFS fitting data is shown in table 4S. LCF-XANES is shown in Figure 5a. CN values from LCF-XANES was determined as follows; Au(I) is taken as $[AuCl_2]^-$ and Au(III) as $[AuCl_4]^-$.

Supplementary Figure 15 – High angle annular dark field (HAADF) images of the 1wt.% Au/C, 1wt.% Pd/C, 1wt.% Pt/C and 1wt.% Ru/C catalysts prepared using acetone at different time-on-line and gas environment.

a) Au/C-Acetone b) Pd/C-Acetone, c) Pt/C-Acetone and d) Ru/C-Acetone catalyst in fresh, after heating to reaction temperature under Ar and after VCM reaction.

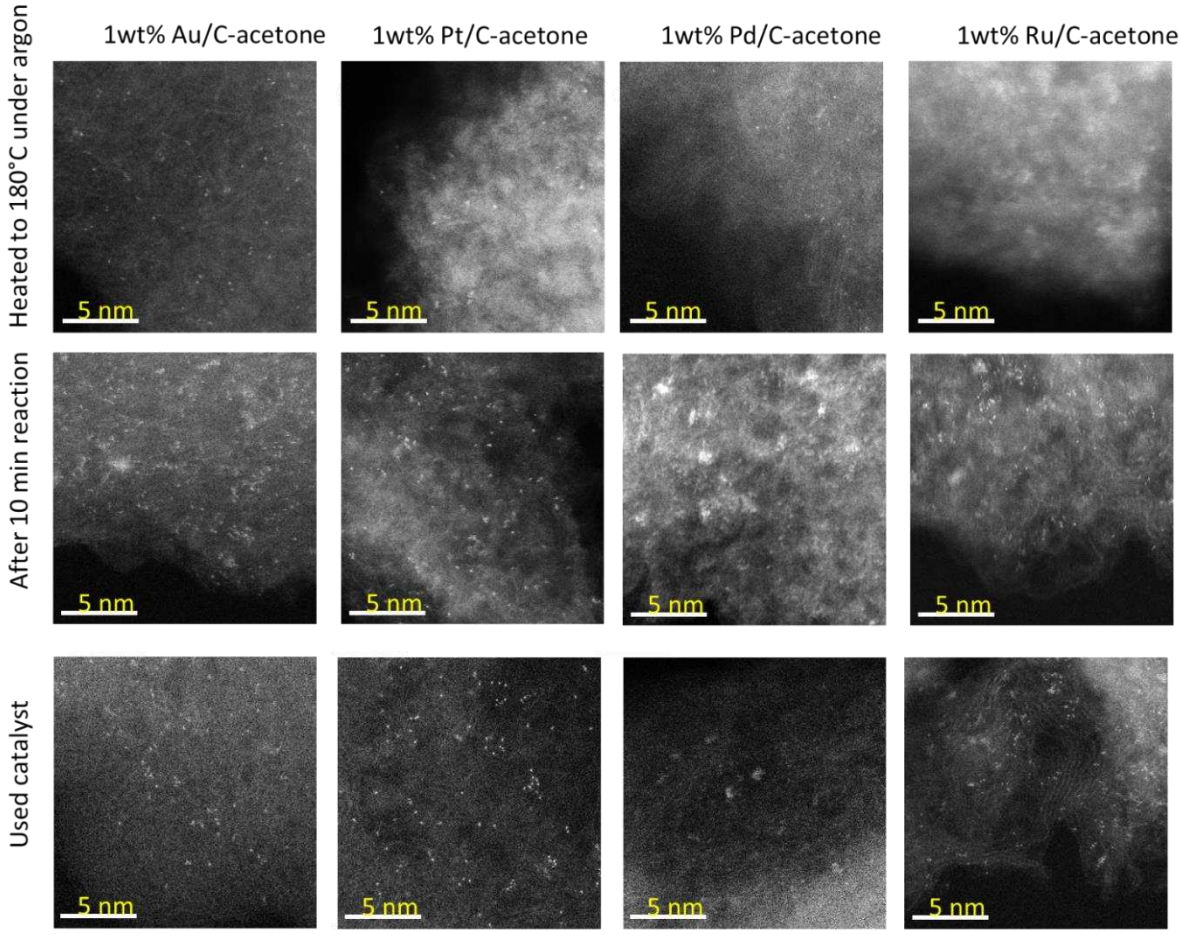

HAADF-STEM shows that the isolated cation sites remain intact apart from a few sub-nanometre clusters visible for the Pd/C and Ru/C samples.

Supplementary Figure 16 – XPS spectra of the 1wt.% Pd/C, 1wt.% Pt/C and 1wt.% Ru/C catalysts prepared using acetone after reaction.
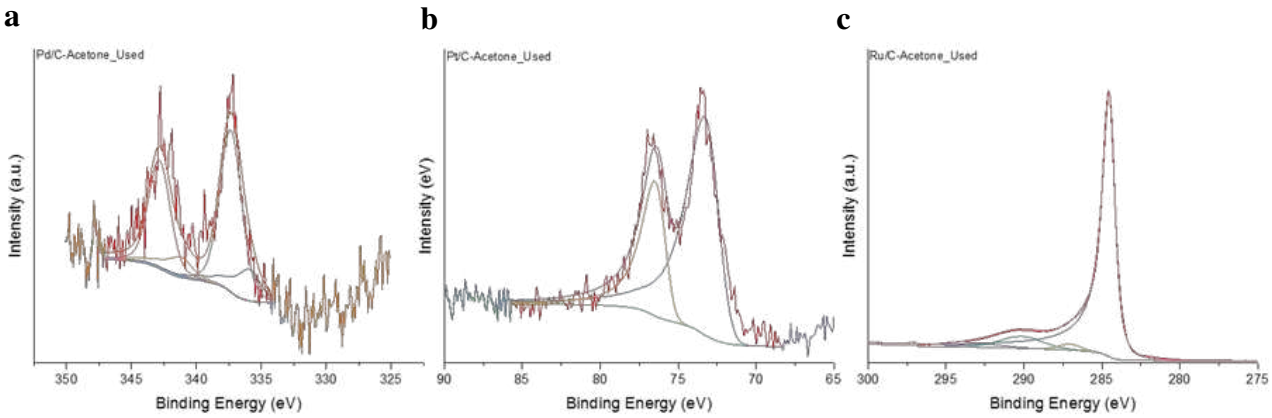
a) 1wt.% Pd/C-Acetone (Pd 3d), b) 1wt.% Pt/C-Acetone (Pt 4f) and c) 1wt.% Ru/C-Acetone (C 1s - Ru 3d).